63 3 4

Investigation of the Conduction Mechanism in Insulating Solids

Contractor: Walter Eric Spear, University of Leicester, Leicester, England.

Contract: DA - 91 - 591 - EUC - 2020

Report: Final Technical Report No 3, November, 1962.

Period: 1st November, 1961 - 30th November, 1962.

The research reported in this document has been made possible through the support and sponsorship of the U.S. Department of Army, through its European Office.

INDEX:

SUMMARY

Fast pulse techniques have been used to study the drift mobility of both electrons and holes in undoped CdS crystals of high resistivity over the temperature range from 500°K to 80°K. A short electron pulse generated free carriers near the top electrode and measurements of the transit time in a pulsed applied field led to a value for the drift mobility. The method is sensitive to the injection of additional carriers and the choice of electrodes is discussed. In the temperature range above about 160°K the electron drift mobility μ_e is in good agreement with Hall mobility values. Below this temperature a transition takes place to a charge transport predominantly controlled by a level of states close to the conduction band. The depth of the centres depends on their density; at infinite dilution it is 0·049ev. Calculated μ_e vs. 1/T curves agree well with the experimental values. It is shown that all the published electron mobility data lie surprisingly close to a mobility curve determined by acoustic mode scattering (μ a $T^{-3/2}$) from 700°K to about 80°K.

The experimental method provides direct evidence for the transport of holes in CdS. At room temperature the hole drift mobility μ_h has a mean value of 15 $cm^2 sec^{-1} v^{-1}$ and the hole lifetime lies between 1×10^{-7}sec and 3×10^{-7}sec. In the lower temperature range all log μ_h vs 1/T curves decrease linearly with an activation energy of 0·019 ± 0·002 ev. An attempt has been made to interpret the results in terms of a model of hole transport in the upper two valence bands of CdS.

In the second part of the report work on the hole transport and the optical absorption in orthorhombic sulphur crystals is described. Details of the crystal growth and the specimen preparation are given. It has been possible to grow thin platelets from solution in CS_2 and the crystallographic orientation of this habit has been determined. Drift mobility measurements on the crystals show that the transport is predominantly by holes which possess a surprisingly long lifetime with respect to deep trapping centres ($\tau_h \sim 20\,\mu$ sec). The temperature dependence of mobility is of the form $\mu_h \propto e^{-\epsilon/kT}$ A possible interpretation is in terms of a hole transport controlled by a level of trapping states about 0·11ev above the valence band. The lifetime of generated electrons is extremely short ($< 5 \times 10^{-9}$sec). Experiments indicate that electrons are trapped in centres lying 0·95ev below the conduction band which possess a comparatively large capture cross section ($\sim 10^{-13}$cm^2).

Absorption measurements between 380 and 500 mμ have been carried out on a number of specimens. As in CdS crystals the position of the edge depends on the orientation of the c-axis with respect to the plane of polarization of the incident light. The experiments show that the absorption edge shifts towards the shorter wavelengths when $E \perp c$-axis The displacement between the edges is about 0·05ev.

During the period covered by this report the research has essentially been concentrated on two main problems. The first, described in Part A of the report, is a fairly detailed study of the transport of electrons and holes in CdS crystals and its temperature dependence. Part B deals with the second problem, an investigation of the hole transport in orthorhombic S crystals and of some of their optical properties.

A. Electron and Hole Transport in CdS Crystals.

§ 1. Introduction.

The widespread use of CdS in photoconductive and other devices has stimulated an interest in some of the fundamental properties of this substance. Although the optical properties have been studied in considerable detail, far less definite information appears to be available on the nature and mechanism of the charge transport in CdS. The first studies of the electron mobility and its temperature dependence in single crystals were carried out by Kröger, Vink and Volger (1954). The results were interpreted in terms of a combination of acoustic and optical mode scattering. In similar experiments by Miyazawa, Maeda and Tomishima (1959) the temperature dependence was explained by optical mode scattering alone, but the effect of impurity scattering was taken into account. Further results were reported by Piper and Halsted (1960); again optical mode scattering was regarded as the predominant mechanism. Piezoelectric scattering was taken into account and led to an improved fit in the low

temperature range. It is evident that there exists considerable disagreement in the interpretation of the electron mobility results. This will be discussed further in § 4 of the report.

All the above experiments were carried out using Hall effect and conductivity measurements and yielded no information on the hole transport in CdS. Yet the work on low field electroluminescence (Smith 1957), the photo-electromagnetic effect (Sommers et al 1956), and other experiments (Diemer and Hoogenstraaten 1956, van Heerden 1957) had led to the general conclusion that holes must be mobile, with a lifetime of 10^{-6} to 10^{-7} sec. It seemed, therefore, that a completely different experimental approach to these problems might prove of some interest. This paper describes the application of drift mobility techniques to the study of carrier transport in CdS, which made it possible to investigate the hole mobility and lifetime in a direct and unambiguous way. Some of the results have already been briefly reported (Mort and Spear 1962); a more complete description of these experiments is given here and an attempt has been made to interpret the temperature dependence of the hole mobility in terms of the valence band structure.

In addition, the temperature dependence of the electron drift mobility has been investigated. These results are of interest in two respects. At temperatures above about 160°K they provide some information on the lattice scattering mechanism; the satisfactory agreement with Hall mobility values in this range is a valuable check on both the experimental method and the interpretation of the measurements.

At lower temperatures, where the drift mobility values are determined by a level of centres close to the conduction band, an analysis of the curves leads to information on the position and density of these centres.

The experimental method is particularly suitable for highly insulating solids and it was possible throughout this work to use 'pure' crystals; by this we mean that no deliberate addition of impurities was made during growth and also that the crystals were not pre-treated in any way before use.

§ 2. Experimental Details.

2.1 Experimental Method.

The method was essentially the same as that used by Spear (1960, 1961) in the study of charge transport in the Se allotropes; it is based on fast pulse techniques which have been more fully described elsewhere (Spear, Lanyon and Mort 1962). A pulse of 40 Kev electrons with a duration of 10 nsec generated free carriers within 5μ of the top electrode. About 2 msec before the arrival of the excitation pulse, a pulse field E was applied across the specimen for a few milliseconds and, depending on the polarity of E, either electrons or holes were drawn into the crystal bulk. The charge displacement caused by the drifting carriers was integrated and displayed on wide band electronic equipment. A specially designed gating unit was used across the amplifier input in order to prevent paralysis. The apparatus was normally run at a repetition frequency of 50 pp sec. The levelling off of the integrated signal marked the arrival of the generated carriers at the bottom electrode and led to a value for the transit time t_t. At each temperature t_t was measured as a function of E. A plot of $1/t_t$ against E, which was found to be linear up to the highest fields used ($\sim 3 \times 10^4$ v cm^{-1}), then led to the drift mobility $\mu = d/Et_t$ where d denotes the specimen thickness.

For the observation of well defined transit times it is important to prevent the appreciable build up of an internal space charge which frequently results from deep trapping. In this connection a useful check consisted in running the excitation pulse and the gate at a frequency of 100 pps and the applied field at 50 pps. Any charge displacement observed with alternate test pulses in absence of the applied field then indicated the presence of an internal space charge field. It was normally possible to eliminate these effects by reducing the carrier generation to below about 10^6 per pulse.

2.2 Specimens, choice of electrodes and specimen mounting

The high resistivity crystals used throughout the investigation were grown from the vapour phase with purified starting materials and ranged in thickness from 50μ to 800μ. They were obtained from three different sources: R.C.A., Princeton; A.E.I., Harlow; E.M.I., Hayes. In the experiments described both the electron and hole mobilities were measured in a direction perpendicular to the c-axis of the crystal.

In the course of preliminary experiments on CdS it soon became apparent that the observation of carrier drift was complicated, and in some cases completely masked, by the presence of secondary effects.

These seemed to be connected with the injection of excess carriers through the electrodes. For this reason the response to the fast excitation pulses of crystals with different electrodes was examined. The pulsed field across the specimen was applied in a direction so as to draw electrons out of the region of excitation. Crystals with In top and bottom electrodes did not show any transit of the generated carriers. This was presumably masked by the heavy injection following the excitation pulse. On the other hand specimens with Au electrodes, which in our experience seemed to be at least partially blocking on CdS, also led to negative results. In this case the reason appeared to be a polarization of the specimen, possibly from the build up of a positive trapped space charge in the region of the top surface. This would tend to decrease, and eventually to annul, the applied field throughout most of the specimen. The observation of pronounced reverse polarization pulses on excitation at 100 c/s supported such an interpretation.

These difficulties were resolved by the use of 'mixed' electrodes. It was found in general that for the observation of well-defined electron or hole transits the top electrode should be blocking and the bottom electrode injecting for the type of carrier making the transit. It appears that in the off-period of the applied field, when both electrodes are at earth potential, a reverse injection through the bottom electrode can take place which reduces the build up of polarizing space charge by recombination. With these electrodes no space charge could be detected on 100 c/s operation for up to 10^6 carriers drifting across

the specimen per pulse. A similar self-neutralisation effect has been observed by Freeman, Kallman and Silver (1961). Further experiments indicated that the blocking top electrodes, gold for electrons, indium for holes, tended to become unstable after prolonged use at elevated temperatures. Because of this uncertain behaviour an artificial blocking electrode, consisting of a 0·5μ blown Pyrex film, was used in most of the experiments. The incident electrons penetrated this electrode with negligible loss in energy.

The method of mounting the crystals is shown in figure 1. The bottom electrode B was stuck to the mica base M by a thin layer of silver paste. In accordance with the above experimental results B consisted of an evaporated In layer for the observation of electron transits; for hole mobility measurements the layer of silver paste itself was used as the bottom electrode. The Pyrex film P, carrying an evaporated Au layer on its top surface, was pressed on to the specimen by a flat metal ring R. This was attached to a simple spring lever which could be gently lowered by turning the screw S so that P made intimate contact with the surface without buckling. Normally the top surface of the specimen also carried a thin evaporated Au layer, left electrically floating, which ensured a uniform surface potential.

§ 3. Experimental Results and their Interpretation.

3.1 Electron Transport

The electron drift mobility μ_e was investigated for six crystals.

The experimental points in figure 2 show the temperature dependence between 500°K and 83°K for three of the specimens, plotted on a graph of log μ_e vs. $10^3/T$. The solid curves were calculated from equation (1). It can be seen that at the higher temperatures the experimental results, particularly for specimen 1, coincide closely with the curve $\mu_L = bT^{-3/2}$; the best fit was obtained with the constant $b = 1{\cdot}28 \times 10^6 cm^2 sec^{-1} v^{-1} o K^{3/2}$. With decreasing temperature, however, μ_e passes through a maximum and then decreases towards the lower temperatures. Both the position of the maximum and the low temperature values of μ_e depend strongly on the specimen.

The temperature dependence of μ_e can be explained in terms of a transition from a lattice controlled to a trap controlled mobility. A very similar behaviour has been observed in monoclinic Se crystals (Spear 1961). In the presence of a level of shallow centres of density N_t, at a depth ϵ below the conduction band, the observed mobility μ_e is given by

$$\mu_e = \mu_L \left[1 + (N_t/N_c) e^{\epsilon/kT}\right]^{-1} \qquad (1)$$

where μ_L is the mobility determined by lattice scattering and N_c is the effective density of states at the bottom of the conduction band. Equation (1) followsdirectly from equation (6) derived in Section 3.2 by putting $\mu_1 = 0$, $\mu_2 = \mu_L$ and $N_1 = N_t$.

In order to apply equation (1) the temperature dependence of μ_L has to be known. On the basis of the experimental results, particularly

those for specimen 1 which correspond to the smallest value of N_t, it will be assumed that the relation $\mu_L = 1{\cdot}28 \times 10^6 T^{-3/2}$ represents the lattice mobility throughout the temperature range considered (see also §4). Charged impurity or defect centre scattering which may contribute at low temperatures has been neglected. The effective electron mass was taken as $m_e^* = 0{\cdot}2m$.

The solid curves in figure 2 show the calculated temperature dependence of μ_e; the agreement over the complete temperature range is very satisfactory and lends support to the above assumptions. The best set of values for N_t and ϵ were obtained by means of an electronic computer and are plotted in figure 3. The graph shows the pronounced decrease of activation energy with increasing density of centres, an effect studied in some detail by Pearson and Bardeen (1949). Their results for boron doped Si specimens could be expressed in the form $\epsilon = \epsilon_o - aN^{1/3}$, where ϵ_o denotes the activation energy at infinite dilution, N the density of ionised donors, and a is a constant. This relation appears to apply equally to the electron traps in CdS as shown by the solid curve in figure 3 which represents the equation $\epsilon = 0{\cdot}049 - 4{\cdot}2\times10^{-8} N_t^{1/3}$. The value of a is in reasonable agreement with that calculated from the theory given by Pearson and Bardeen.

The room temperature values of μ_L obtained from all the specimens lie close to 265 $cm^2 sec^{-1} v^{-1}$. This is in satisfactory agreement with the Hall mobility results (see figure 8, §4. and

compares well with the drift mobility value of 285 $cm^2 sec^{-1} v^{-1}$ recently obtained by Hutson et al (1961) using a completely different experimental technique.

3.2 Hole Transport

As mentioned in § 2.2 the drift of the generated holes could be observed provided suitable specimen electrodes were used. Unlike the electron pulses the observed pulse shapes for holes clearly showed the influence of deep traps. These centres, which may well be connected with the recombination process, possess a thermal release time far longer than the transit time. At low applied fields ($E \lesssim 4 \times 10^3$ v cm^{-1}) this resulted in an appreciable loss of carriers during transit and the pulse shape shown in figure 4a was observed. At higher fields (figure 4b) the rising edge of the pulse tended to become practically linear suggesting that t_t had now become shorter than the hole lifetime τ_h associated with these centres.

From the experimental point of view it was convenient to introduce a time t' defined by the intersection of the tangents to the pulse at t = 0 and $t \gtrsim t_t$. In the presence of a uniform volume distribution of deep lying hole traps the charge displacement is given by the well known Hecht formula (Hecht 1932):

$$q(t) = (Ne\mu_h E\tau_h/d)\left[1 - \exp(-t/\tau_h)\right] \quad \text{for } t \leq d/\mu_h E \qquad (2)$$

where N denotes the total number of holes per pulse drawn out of the

surface region. The tangent at t = 0 is therefore given by $q'(t) = Ne\mu_h Et/d$. At $t = t_t = d/\mu_h E$ the total charge displacement is

$$Q(t_t) = (Ne\mu_h E\tau_h/d)[1 - \exp(-d/\mu_h E\tau_h)]$$

At the point of intersection, $q'(t') = Q(t_t)$, leading to

$$1/t' = (1/\tau_h)[1 - \exp(-d/\mu_h E\tau_h)]^{-1} \quad \text{—(3)}$$

The hole mobility at room temperature was investigated in seven crystals all of which showed the same general behaviour. In figure 5a, b and c, the experimental values of 1/t' are plotted against E/d for one crystal from each source. According to equation (3), $t' = \tau_h$ at E/d = 0, and τ_h could be obtained from the graph. With the known value of τ_h, t_t was calculated from equation (3) for each experimental point. This led to the $1/t_t$ curves shown in figure 5 from which μ_h was obtained. The good linearity of the calculated curves supports the validity of equation (3). The room temperature values of μ_h for the seven crystals lie between 10 and 18 $cm^2 sec^{-1} v^{-1}$ with a mean value of about 15 $cm^2 sec^{-1} v^{-1}$. The spread in the mobility values arises partly from the difficulty of measuring the local crystal thickness in the bombarded area. The hole lifetimes ranged between 1×10^{-7} sec and 3×10^{-7} sec in agreement with the estimates referred to in §1.

The temperature dependence of μ_h was investigated from 500°K to 77° for five of the specimens. The results are shown in figure 6.

The mobilities have been normalised to the room temperature value $(\mu_h)_r$ to facilitate correlation of the results for the different specimens. The graph shows that μ_h varies in a similar way to μ_e in that it exhibits a maximum and decreases exponentially in the lower temperature range. However, in striking contrast to the electron curves, the results for all five specimens now lie close to a common curve. Below about 170°K the the log μ_h versus 1/T curve for all the specimens decreases linearly with an activation energy of 0·019 ± 0·002 ev. An interpretation of these results in terms of a trap controlled mobility would require the remarkable coincidence that five specimens from three different sources possessed an identical density of traps. In view of the electron results this would seem unlikely, particularly as the shape of the mobility curve is sensitive to the trap densities, and comparatively small differences in N_t should have been detected. Further evidence against an interpretation of the hole mobility curve in terms of a trap controlled mechanism is the fact that all attempts to produce p-type CdS have been unsuccessful.* As far as is known to the authors no defect or impurity levels lying closer than about 0·16 ev to the valence band have been reported. These considerations point therefore towards an interpretation of the hole mobility results in terms of a more fundamental property of CdS.

The dichroism in the optical absorption edge of CdS was first observed by Gobrecht and Bartschat (1953) and has since been confirmed by other workers. The experiments indicate that the separation of

* It should be mentioned in this connection, that Woods and Champion (Journal of Electronics and Control 7, 243, 1959) have observed a positive Hall coefficient on highly doped CdS. Their crystals contained about 5×10^{20} Cu atoms p. cm^3 and it is likely that the observed hole transport is associated with the Cu impurity band.

the two edges obtained with light having its E-vector parallel and perpendicular to the crystal c-axis is about 0·020ev, decreasing to 0·016evat 4·3°K.

The dichroism has been explained in terms of the valence band structure by the group symmetry studies of Birman (1959), Balkanski and des Cl·izeaux (1960) and others. It is shown that the effect of the crystalline field and of spin orbit coupling leads to three non-overlapping bands near the centre of the Brillouin zone as indicated in figure 7. Optical excitation from band 1 to the conduction band can take place only if the absorbed light is polarized with its E-vector perpendicular to the c-axis, whereas transitions from band 2 are allowed for both planes of polarization. According to this model, the energy separation between the upper two bands should therefore be about 0·020ev. The close agreement with the activation energy of 0·019ev found in our experiments suggests that the observed temperature dependence below about 170°K may be connected with transitions of free holes between bands 1 and 2.

On this basis the following expression for the charge transport can be derived. If μ_1 and μ_2 are the lattice mobilities in the two bands and p_1 and p_2 the corresponding hole densities, then

$$\mu_1 (p_1 + p_2) = \mu_1 p_1 + \mu_2 p_2 \qquad (4)$$

on the assumption that the classical thermal equilibrium distribution can be used to describe the carrier densities during transit,

$$p_1 / p_2 = (N_1 / N_2) \exp(\Delta\epsilon / kT) \qquad (5)$$

where $\Delta\epsilon = 0{\cdot}019$ev according to our results. Substitution of equation (5) into (4) then leads to

$$\mu_h = \mu_2 \left[1 + bN\exp(\Delta\epsilon/kT)\right]\left[1 + N\exp(\Delta\epsilon/kT)\right]^{-1} \qquad (6)$$

where b denotes the mobility ratio μ_1/μ_2 and N the density of states ratio N_1/N_2.

In view of the unknown parameters b, N and μ_2 only a few tentative deductions can be made. These are based on the experimental fact that $\mu_h \propto \exp(-\Delta\epsilon/kT)$ for $T \leq 170^{\circ}K$. According to equation (6) this can be satisfied if (i) $N\exp(\Delta\epsilon/kT) \gg 1$, and (ii) $\mu_2\left[1 + bN\exp(\Delta\epsilon/kT)\right]$ is practically temperature independent in the range $170^{\circ}K > T > 77^{\circ}K$. Various attempts at curve fitting indicated that apart from satisfying (i) a value of $N \geq 5$ is needed to provide even an approximate fit. The second condition implies that μ_2 has to be combined with a scattering mechanism which leads to a decreasing mobility with decreasing T. This would occur if charged impurity or defect scattering were present. However, a large density of such centres ($\sim 10^{18}$cm^{-3}) has to be assumed to give a sufficiently shallow maximum in μ_2 within the specified temperature range. On the assumption of spherical energy surfaces the condition $N \geq 5$ implies that $m_1^*/m_2^* \geq 3$. This indicates that $\mu_2 > \mu_1$, so that band 2 is the fast band.

3.3. Ambipolar Diffusion

Since electron and hole drift mobilities are now known from

direct measurements it is possible to calculate a value for the ambipolar diffusion constant D_a. For an insulating crystal in which the thermal equilibrium carrier density is much smaller than the density of generated carriers, $D_a = [2\mu_e\mu_h/(\mu_e+\mu_h)]\,kT/e$ (Diemer and Hoogenstraaten 1957). With μ_e = 265 $cm^2sec^{-1}v^{-1}$, μ_h = 15 $cm^2sec^{-1}v^{-1}$, D_a = 0·71 cm^2sec at room temperature. Using $\tau_h = 2 \times 10^{-7}$sec, the ambipolar diffusion length $\ell_a = 3{\cdot}7 \times 10^{-4}$cm. This value of ℓ_a is in reasonable agreement with the estimate by Auth (1961) based on P.E.M. effect measurements. A further rather critical test of the consistency of our results is provided by the P.E.M. measurements of Sommers et al (1956) who obtained a value of $\mu^{*3}\tau_h \simeq 1 cm^6sec^{-2}v^{-3}$ at room temperature for highly insulating CdS crystals. μ^* is an ambipolar mobility which should be replaced by $2\mu_e\mu_h(\mu_e+\mu_h)$. With our data, $\mu^{*3}\tau_h$ = 0·5 $cm^6sec^{-2}v^{-3}$, so that the agreement between values obtained by completely different experimental methods is reasonable.

§4. Discussion

The electron mobility results given in figure 2 showed that a $T^{-3/2}$ temperature dependence, normally associated with non-polar acoustic mode scattering, provides a good fit to the experimental curves. This result is surprising because the bonding in the wide gap II-VI compounds, such as ZnS and CdS, is generally throught to be

partly ionic. It is of interest in this connection to compare the results of the different electron mobility studies that have so far been carried out. It is evident from figure 8 that the above conclusion is not confined to our own results. The points of both Kröger et al and of Miyazawa et al are evidently in close agreement over most of the temperature range with the curve $\mu = 1\ 28 \times 10^6 T^{-3/2}$ (curve 1 in figure 8) used in the interpretation of our results. The mobility values given by Piper and Halsted for their undoped specimens lie consistently higher than the other results, but they also can be described convincingly by a $T^{-3/2}$ temperature dependence from 700°K to 80°K (curve 2: $\mu = 2{\cdot}0 \times 10^6 T^{-3/2}$). The curve marked μ_o represents the mobility determined by optical mode scattering. It is identical with that used by Piper and Halsted and has been calculated from the formula given by Petritz and Scanlon (1955) with a characteristic temperature of $\Theta = 440°K$ (Collins 1959) for the longitudinal optical phonons. It should be noted that μ_o deviates markedly from all experimental curves above room temperature, and increasingly so towards the higher temperatures. This would be difficult to understand if polar scattering were the predominant mechanism. In that case one would expect a progressively closer fit at temperatures approaching and exceeding Θ. These considerations throw some doubt upon the interpretations that have so far been given. One may conclude at this stage that either acoustic mode scattering is the predominant

mechanism, or that the theory of optical scattering in its application to CdS requires some refinement, possibly along the lines developed by Ehrenreich (1957, 1959) for InSb.

In our high resistivity crystals the shallow electron traps are most probably connected with an almost completely compensated donor level. The nature of these centres is still uncertain. They could be due to impurities in the starting materials, or, alternatively, they might be associated with a definite type of crystal defect caused by non-stoichiometry in the composition of the crystals. A singly ionised sulphur vacancy would be an example of this second possibility. As has been shown by the extensive work of Kröger, Vink and van den Boomgaard (1954), the activation energies associated both with donor impurities and with shallow defect centres are about 0·03ev. Using the hydrogen orbit approximation Kröger et al estimated a value of $\in$ = 0·04ev with m_e^* = 0·2m, which agrees approximately with the value found in §3.1. As drift mobility experiments at the lower temperatures provide a sensitive means for studying shallow centres, it would be of interest to extend these experiments to doped specimens or to crystals grown under conditions which produce a known type of defect.

In connection with the hole transport measurements, our conclusion μ_2 μ_1 disagrees with the calculations of Hopfield (private communication). From a perturbation calculation Hopfield estimated a nearly isotropic value of $m_2^* \simeq 1{\cdot}0m$ based on the data for band 1.

obtained from magneto-optical experiments (Hopfield and Thomas 1961). These gave a value of $m_1^* \simeq 0{\cdot}7m$ (perpendicular to the c-axis) which would suggest that, contrary to our conclusions, μ_1 is somewhat larger than μ_2. At present the reason for this disagreement is not clear and further work is in progress to show whether or not our tentative conclusion is valid.

Acknowledgments

The authors wish to thank Dr. R.W. Smith of R.C.A., Dr. J. Franks of A.E.I. and Mr. E. McGill of E.M.I. for kindly supplying the crystals used in this work. We are indebted to Professor J.J. Hopfield for unpublished effective mass data and to Dr. A. Weinmann for help with the computer programme.

B. Some Electrical and Optical Properties of Ortho-rhombic Sulphur Crystals.

§ 1. Introduction.

During the last sixty years a considerable number of papers have appeared dealing with the physical properties of the various forms of sulphur. As for the electrical properties, most of the earlier work was concerned with measurements of resistivity, the rise and decay of currents and the associated charge storage effects. This work gave little definite information on the more fundamental aspects of the charge transport in this solid.

In a recent paper Dean, Royce and Champion (1960) described experiments on the induced conductivity in ortho-rhombic S crystals under α-ray bombardment using counting techniques. The results are of considerable interest, but their interpretation in terms of fundamental parameters is complicated. On the basis of the present work we disagree with some of the main conclusions drawn by Dean et al. This will be discussed further in §4.3.

The application of drift mobility techniques to S was suggested in the original research proposal in 1959, but the work was started only about one year ago. Optical equipment had by then become available and it was felt that the correlation of electrical and optical experiments on the same specimens would lead to a more complete understanding of the conduction process.

§ 2. Crystal Growth.

Most of the crystals used in this investigation were grown from solution in carbon disulphide. A number of attempts have been made to grow crystals from the vapour phase at a pressure below the triple point ($3{\cdot}7 \times 10^{-3}$ mm of Hg). However, the crystals obtained so far by this method were too small for use.

Growth from solution was carried out under the following two conditions: (a) by cooling of the saturated solution in a closed vessel and (b) by slow evaporation of the solution at a constant temperature. Method (a) led normally to fairly large thick crystals in the shape of a pyramid, shown in figure 9. This is a well known habit of rhombic S (e.g. see Berry and Mason 1959) and the crystalline axes can easily be recognised.

The most convenient shape for electrical and optical studies is a flat crystal plate and some effort was made to grow thin S platelets. It was found that method (b) led to this type of specimen. As shown in figure 10, a pool of a nearly saturated solution is spread on to a horizontal glass plate of about 8" diameter. This was kept in a constant temperature enclosure and the rate of evaporation could be controlled by the diameter of the glass tube in the lid of the enclosure. By allowing complete evaporation of the solvent in one day, about 40 platelets of approximately 5mm sidelength were obtained which ranged in thickness between 200 μ and 500 μ. Their typical shape is shown in figure 11.

To identify this habit a polarising microscope in conjunction with a universal stage specimen holder was used. The position of the achromatic lines of the birefringent crystal showed that the c-axis makes an angle of 18° 20' with the crystal face. This is therefore a (111) plane and corresponds to face A of the pyramid habit shown in figure 9. This conclusion and the ortho-rhombic structure of the crystals have been confirmed by a number of Laue and Oscillation X-ray photographs. Some diffuse scattering was observed which may be due to strain in the crystals; it is planned to investigate the effect of a careful annealing treatment.

§ 3. Specimen Preparation.

Crystals were grown from both ultra-pure and ordinary laboratory reagents. For the first group, Light's ultra-pure S (99·999% minimum purity) and 'infra-red' grade CS_2 was used. So far the mobility measurements have been confined to the thin crystal plates, but it seemed of interest to investigate optical properties along different orientations. For this purpose it was attempted to suitably grind and polish some of the pyramid crystals. By means of accurately machined jigs the crystal could be ground either in a plane containing the c-axis or perpendicular to it. Because of the softness of the crystal only the finest grade of carborundum powder (No. 500) was used. The ground platelets were then polished on a slow wheel with a nylon cloth and alumina powder in water.

Initially the crystals were fitted with evaporated Au electrodes. But painted electrodes of colloidal graphite in alcohol were found to be very satisfactory and were used in most of the subsequent experiments. Fine connecting wires were attached with silver paste. The small deposit of silver sulphide which formed around the joint after a few days did not appear to affect the electrical properties.

§ 4. Mobility Measurements.

4.1. Hole Mobility.

The fast pulse methods briefly described in part A, § 2, were applied to the study of carrier mobilities in the sulphur cystals. Beaause of the longer transit times it was possible to use excitation pulses of 90 nsec duration.

Well defined hole transits were observed in all crystals, whether prepared for ultra-pure reagents or not. The linearity of the oscilloscope trace, representing the integrated charge displacement of the drifting carriers, indicated that except at very low applied fields, the loss of holes into deep traps was negligible. For transit times in excess of about 20μsec a deterioration in the pulse shape was normally observed. This indicated that the hole lifetime with respect to deep traps is of that order. The measurements were generally carried out using a pulsed applied field (50 p.p. sec) and an exciting beam pulsed at 100 p.p. sec. (see part A § 2.1); this provided a certain amount of space charge neutralisation. A transit pulse of considerably reduced amplitude could even be observed with a steady applied field.

Figure 12 shows a typical graph of $1/t_t$ vs. V, the potential applied across the crystal. The specimen, S23, originally 420μ thick, was selected from a batch grown with ordinary laboratory reagents. Curve (1) shows the initial results leading to a hole drift mobility $\mu_h = 2{\cdot}0\ cm^2 sec^{-1} v^{-1}$. The intercept with the V-axis is most likely connected with a sheet of negative space charge near the top electrode; a similar effect has been found in vitreous Se (Spear 1957). Curve (2) was obtained after grinding first the bottom and then the top of the crystal and re-applying electrodes to the ground faces. The value of μ_h calculated from the new thickness (330μ) was still $2{\cdot}0\ cm^2 sec^{-1} v^{-1}$, indicating that transport measurements on S are not affected by ground faces. This conclusion is of importance in the planned investigation of hole mobility along different crystallographic directions in which the of ground crystals will be essential.

Figure 14 shows the temperature dependence of μ_h. The temperature range is limited by the fact that the crystals begin to sublime (in vacuum) above about 50°C and space charge effects obscure the transit below about -100°C.

It can be seen that all the specimens grown from highly purified reagents lie close to line (1) and give a room temperature mobility of about $0{\cdot}4\ cm^2 sec^{-1} v^{-1}$. The other specimens lead to consistently higher mobilities. Although there is some considerable spread in the values from different specimens, the temperature dependence of this group can be approximately represented by line (2) which has the same gradient as (1).

An interpretation of the temperature dependence of μ_h can be given using the model of a trap controlled drift mobility which leads to equation (1) (part A, § 3.1).

If $(N_t/N_v)\exp(\epsilon/kT) \gg 1$, then (1) reduces to

$$\mu_h = \mu_L (N_v/N_t)\, e^{-\epsilon/kT} \qquad (7)$$

From the gradient of the experimental curves it can then be concluded that the level of centres controlling the hole transport lies $\epsilon \simeq 0{\cdot}11$ ev above the valence band. It should be stressed, however, that the evidence in favour of this model is by no means as conclusive as it was in the case of CdS where a clear transition from a lattice to a trap controlled mobility could be observed. There is no indication of a mobility maximum in the results for S. Other models, such as an interpretation in terms of a 'hopping' process, which also leads to a depence of the form $\mu \propto e^{-\gamma/T}$, cannot therefore be excluded.

4.2 Electron Trapping.

No charge displacement that could be associated with the drift of generated electrons has so far been detected. It is therefore likely that the lifetime of electrons with respect to deep traps, τ_e, is shorter than the response time of the equipment. This would indicate a value of $\tau_e \leq 5 \times 10^{-9}$ sec.

A few preliminary experiments have been made to obtain some information about these centres. The crystal is first irradiated with an intense beam of electrons for about 10 sec and a negative potential is applied to the top electrode. It is assumed that under these conditions the electron traps are substantially saturated. Both electrodes are then earthed and the trapped negative space charge is probed after a time t by a small electron pulse. The amplitude h_t of the observed displacement pulse of generated holes is taken as a measure of the density of the trapped negative charge. It was found that the results are in agreement with the relation

$$h_t = h_o e^{-t/\tau_r} \qquad (8)$$

where ho denotes the height of the probe pulse at t = 0 and τ_r is the average time an electron spends in the trapping centre. At room temperature $\tau_r \simeq 32{\cdot}5$ mins. whereas at 33°C τ_r has decreased to about 9·5 mins.

It can be shown that

$$\tau_r = \left(N_c \upsilon_{th} \sigma\right)^{-1} e^{\epsilon_t/kT} \qquad (9)$$

where N_c denotes the effective density of states in the conduction band, υ_{th} the thermal velocity, σ the cross section of the trapping centres situated E_t ev below the band. From (9) E_t is found to be 0·94ev. Assuming $m^* = m$ in the calculation of N_c, the value of σ is about 10^{-13} cm^2. One would expect such a comparatively high capture cross section

to be associated with charged centres which exert a Coulomb attraction on the free electrons. With the known value of σ and the estimated value of $\tau_e \leq 5 \times 10^{-9}$sec, $N_t \geq 10^{14}$cm^{-3}. It might be added that the extremely long trapping times for electrons together with the long free lifetimes of holes could be of interest in connection with charge storage or memory devices.

4.3. Comparison with the results of Dean et al.

The main disagreement between our results and those of Dean et al. lies in their conclusion that electrons are the carriers responsible for conduction. This is based on the observation that conduction pulses from the incident α-particles could only be obtained from a sensitive region within 2×10^{-2}cm of the negative electrode. Undoubtedly strong space charge effects complicate the interpretation of the results and the authors apply a theory by van Hippel et al.(1953) originally developed to explain the photoconductivity in alkali halides containing anion vacancies.

It seems to us that the above, and other observations could equally well be interpreted in terms of the drift of generated holes towards the negative electrode. In fact Dean et al. state that the threshold applied field for the observation of counting pulses lay between 5 and 10 kv cm^{-1}. At 5kv cm^{-1} the range of holes would be about 10^{-1}cm using our values of $\mu_h \simeq 1$ cm^{2}sec^{-1}v^{-1} and $\tau_h \simeq 20\mu$sec. This is not inconsistent with the quoted extent of the sensitive region, particularly

as the trapped negative space charge in this region would tend to reduce the internal field below the value V/d.

Our conclusion that holes are the predominant charge carriers is based on the direct observation of the sign of the hole transit pulse. One might argue that we could be looking at electrons moving across the excited region towards the positive electrode. This is unlikely because (a) the mobility calculated from $\mu = d/E t_t$ should then depend on the crystal thickness which certainly is not the case and (b) the value of t_t should depend on the average depth of penetration of the incident electrons. This has been investigated for incident electron energies between 5 and 35kev, the results leading to a constant value of t_t.

Dean et al. have also investigated the decay of the internal space charge after strong illumination. From the temperature dependence of this effect the depth of the centres is found to be 0·92ev in good agreement with our value.

§ 5. Optical Absorption Measurements.

5.1. Unpolarised Light.

The absorption edge of a number of crystals (between 75μ and 750μ thick) has been studied by means of a grating monochromator in the wavelength range from 380mμ to 500mμ. The results for five crystals are given in figure 13. At the higher absorption levels narrow band filters were used to cut out stray light of longer wavelength. So far no

reflection correction has been applied to these measurements. It can be seen that the absorption edge is practically exponential up to the highest absorption level that could be measured with a 75μ thick crystal. On the same graph curve P represents the photoconductive response (in arbitrary units) obtained by Kurrelmeyer (1927) with a natural crystal of Sicilian sulphur. According to the criterion used by Moss (1952) the photoconductive edge should lie near 510mμ corresponding to 2·43ev. A similar value can be obtained from the photoconductivity curves of Tartakovsky and Rekalova (1940). It is most likely that our absorption curve represents the intrinsic edge. The photoconductivity observed by the above workers seems therefore not to be an intrinsic process but may be connected with excitation from impurity or defect centres. Attempts have been made to observe photoconductivity with our crystals using a sensitive vibrating reed electrometer and an intense light source. No signal has been detected so-far.

For an intrinsic process, the equilibrium carrier density should be

$$n = p = 2\left(\frac{2\pi kT m^*}{h^2}\right)^{3/2} e^{-E_g/2kT} \qquad (10)$$

The quoted values for the conductivity of rhombic S vary considerably. More recent measurements, carried out in vacuum and using more reliable electronic instruments, generally lead to lower values for σ. According to the new edition of Kaye and Laby (1956), $\sigma = 5 \times 10^{-24}\ (\Omega cm)^{-1}$. From equation 10 with $m^* \simeq m$ and a mean value of $\mu_h \simeq 1\ cm^2 sec^{-1} v^{-1}$, E_g is

found to be 2·75ev. Neglecting any difference between thermal and optical activation energies, the absorption edge should lie near 450mμ. This is not inconsistent with the measurements shown in figure 15.

5.2. Polarised Light.

A number of experiments have been carried out to investigate the dependence of the absorption edge on the plane of polarisation of the incident light with respect to the crystal c-axis. For this purpose several of the thicker crystals were ground along a plane containing the c-axis and subsequently polished (§3). In all cases the edge was found to depend on the direction of the E-vector, moving towards shorter wavelengths when E was perpendicular to the c-axis. Figure 16 shows a typical set of results. The mean separation amounts to about 0·05ev. As a check a crystal was ground perpendicular to the c-axis. In this case the two edges coincided within experimental error. The observed dichroism in S may well be connected with the band structure, as has been established in the case of CdS or ZnS. It would be of interest if it were possible to extend these group theoretical calculations to an ortho-rhombic structure.

§6. Research Plans.

The results obtained so far are encouraging and it is proposed to carry on this work along the following lines:

(1) Investigation of μ_h along different crystallographic directions.

(2) Mechanism of charge transport: Trap controlled or 'hopping' process?

(3) The properties of doped crystals; possibility of introducing a sufficient density of donars to saturate the 0·94ev level and thus increase the electron lifetime.

(4) Growth of mixed S-Se crystals.

(5) What is the reason for the apparent absence of photoconductive response in our crystals? Comparison with measurements on natural crystals.

(6) Further work on the dichroism of the absorption edge.

REFERENCES FOR PART A.

Auth. J., 1961, Z. Phys. Chem., 217, 159.

Balkanski. M. and des Cloizeaux. J., 1960, J. Phys. Radium, 21, 825.

Birman. J.L., 1959, Phys. Rev., 114, 1490.

Collins. R.J., 1959, J. App. Phys., 30, 1135.

Diemer. G. and Hoogenstraaten. W., 1956, Physica 22, 172.

" " 1957, J. Phys. Chem. Solids, 2, 119.

Ehrenreich. H., 1957, J. Phys. Chem. Solids, 2, 131.

" 1959, ibid, 2, 129.

Freeman. J.R., Kallman. H.P., and Silver. M., 1961, Rev.Mod.Phys., 33, 553.

Gobrecht. H. and Bartschat. A., 1953, Z. Phys., 136, 224.

Hecht. K., 1932, Z. Phys., 77, 235.

Hopfield. J.J. and Thomas. D.G., 1961, Phys. Rev. 122, 35.

Hutson. A.R., McFee. J.H. and White. D.L., 1961, Phys. Rev. Letters, 7, 237.

Kröger. F.A., Vink. H.J. and van der Boomgaard. J., 1954, Z. Phys. Chem., B203, 1.

Kröger. F.A., Vink. H.J. and Volger. J., 1954, Physica, 20, 1095 (referred to as Kroger et al).

Miyazawa. H., Maeda. H. and Tomishima. H., 1959, Phys. Soc. Japan, 14, 41.

Mort. J. and Spear. W.E., 1962, Phys. Rev. Letters, 7, 314.

Pearson and Bardeen, J., Phys. Rev., 75, 865.

Petritz. R.L. and Scanlon. W.W., 1955, Phys. Rev. 97, 1620.

Piper. W.W. and Halsted. R.E., 1960, Proc. Int. Con Semiconductor Phys., Prague, P.1046.

Smith. R.W., 1957, Phys. Rev., 105, 900.

Sommers. H.S., Berry. R.E. and Sochard. I., 1956, Phys. Rev., 101, 987.

Spear. W.E., 1960, Proc. Phys. Soc., 76, 826. also F.T.R.1.

" 1961, J. Phys. Chem. Solids, 21, 110. also F.T.R.2.

Spear. W.E., Lanyon. H.P.D., and Mort. J., 1962, J. Sci. Instr. 39, 81, and F.T.R.2.

Van Heerden. P.J., 1957, Phys. Rev., 106, 468.

References: Part B.

Berry and Mason, 1959, Mineralogy, San Francisco: Freeman & Co.

Dean, Royce and Champion, 1960, Proc. Phys. Soc. 75, 119.

V. Hippel, Gross, Gelatis and Geller, 1953, Phys. Rev. 91, 568.

Kaye and Laby, 1956, Tables of Physical Constants, London: Longman's & Co.

Kurrelmeyer, 1927, Phys. Rev. 30, 893.

Moss, 1952, Photoconductivity, London: Butterworth.

Spear, 1957, Proc. Phys. Soc. 70B, 669.

Tartakovsky & Rekalova, 1940, J. exp. theor. Phys. 10, 1025.

Administrative Details.

Personnel: W.E. Spear.

J. Mort, Research Student at Leicester University until August, 1962.

A. Adams, Research Student at Leicester University.

Hours spent on Contract:

W.E. Spear	about	700 hours.
J. Mort	"	1200 "
A. Adams	"	1200 "

Expenses for materials: about £350.

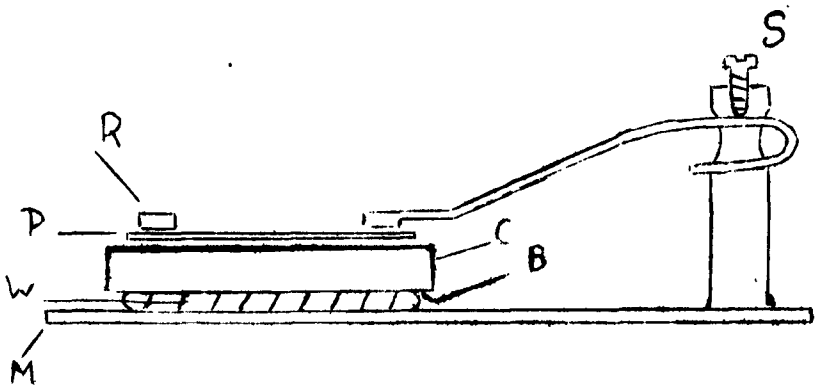

Figure 1: Method of specimen mounting. M, mica base; W, connecting wire; B, bottom electrode; C, crystal; P, pyrex blocking electrode; R, metal ring; S, adjusting screw.

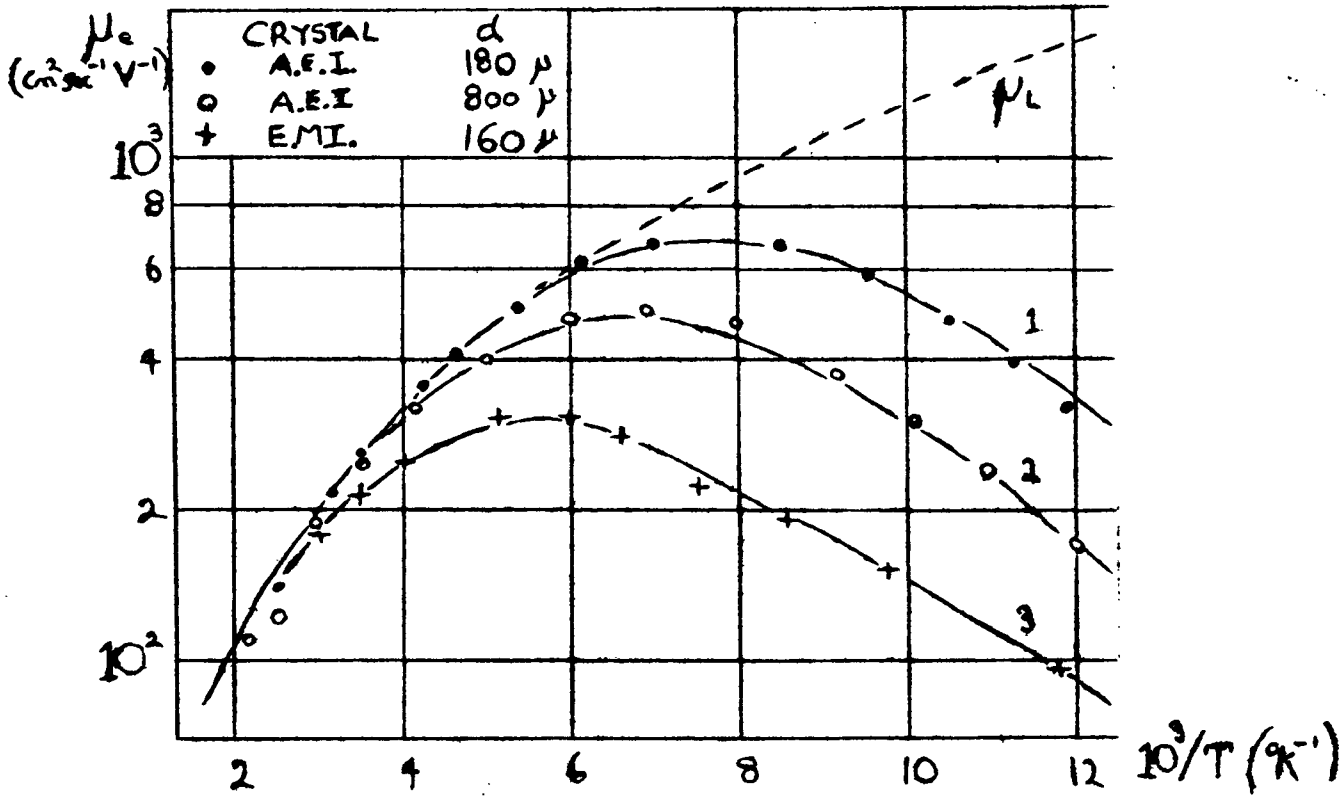

Figure 2: Temperature dependence of the electron drift mobility, μ_e, for three typical specimens. Solid lines were calculated from equation (1). Broken line represents $\mu_L = 1{\cdot}28 \times 10^6 T^{-3/2}$.

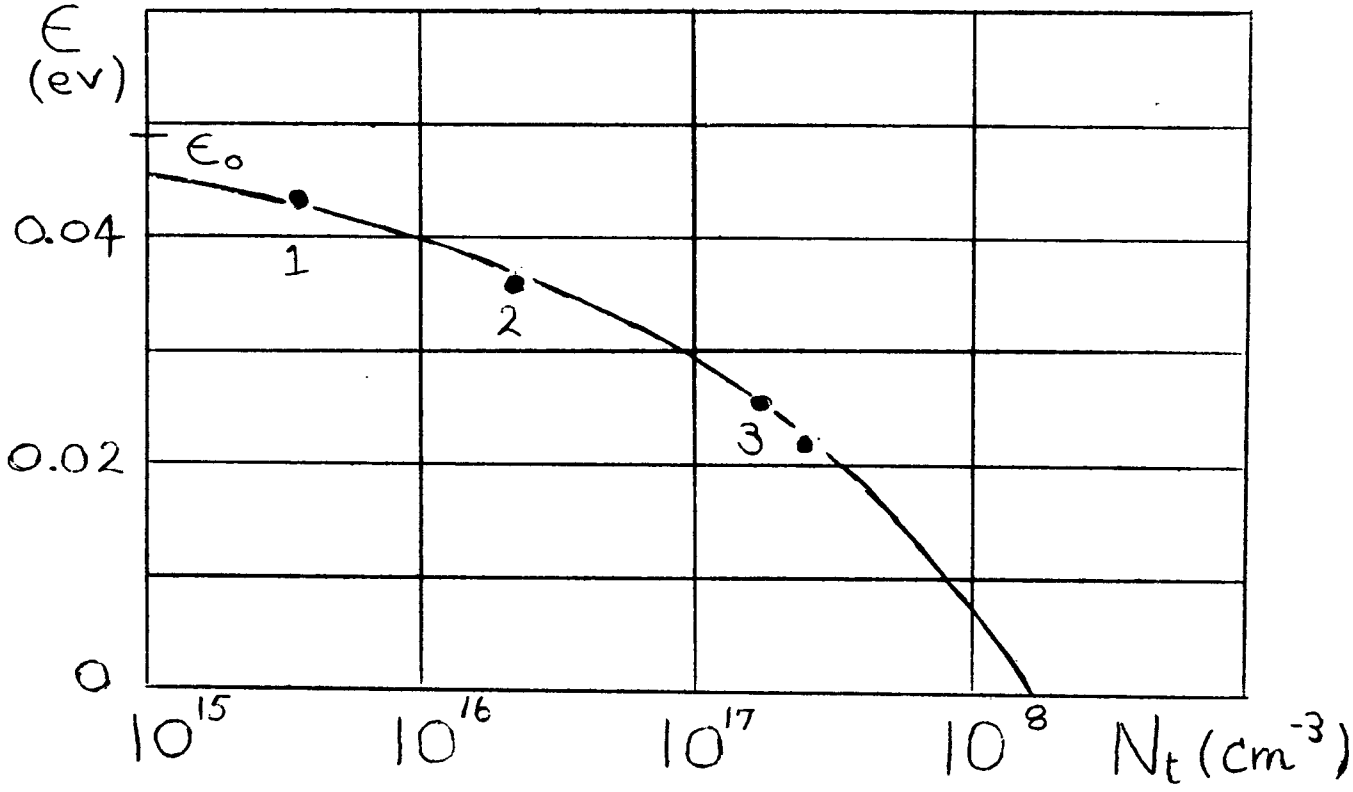

Figure 3: Dependence of electron trap depth ϵ on trap density N_t.

The numbered points refer to the corresponding curves in figure 2.

The solid line represents $\epsilon = \epsilon_0 - aN_t^{1/3}$ with $\epsilon_0 = 0{\cdot}049$ev and $a = 4{\cdot}2 \times 10^{-8}$ cm^{-1}ev

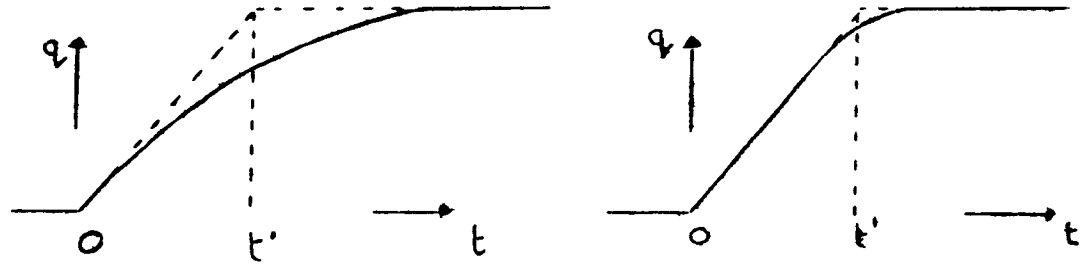

Figure 4: Observed pulse shapes representing the integrated charge displacement when generated holes drift across the specimen.

(a) with low applied field, $E \simeq 4 \times 10^3$ v cm^{-1}, so that $t_t \simeq 2\tau_h$,

(b) with larger field, $E \simeq 1\ 3 \times 10^4$ v cm^{-1}, corresponding to $t_t \simeq \frac{1}{2}\tau_h$.

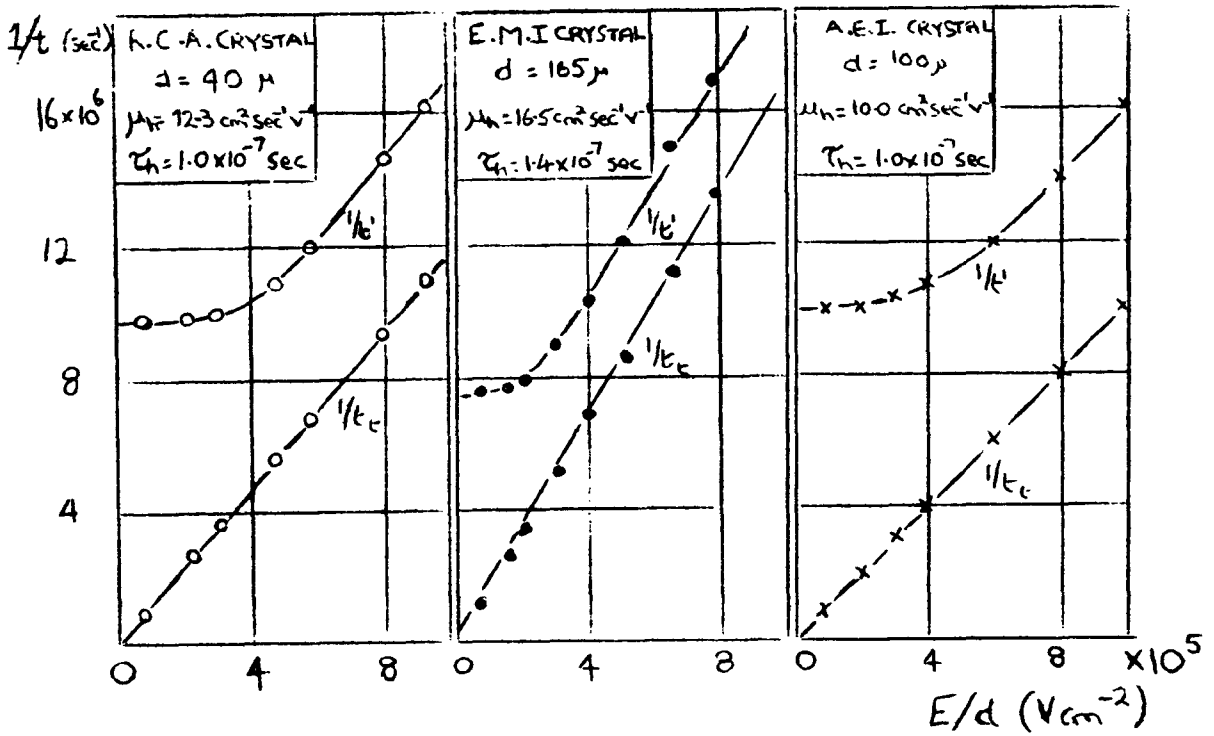

Figure 5 (a), (b), (c): Curves 1/t' and $1/t_t$ vs E/d for three specimens from the sources indicated.

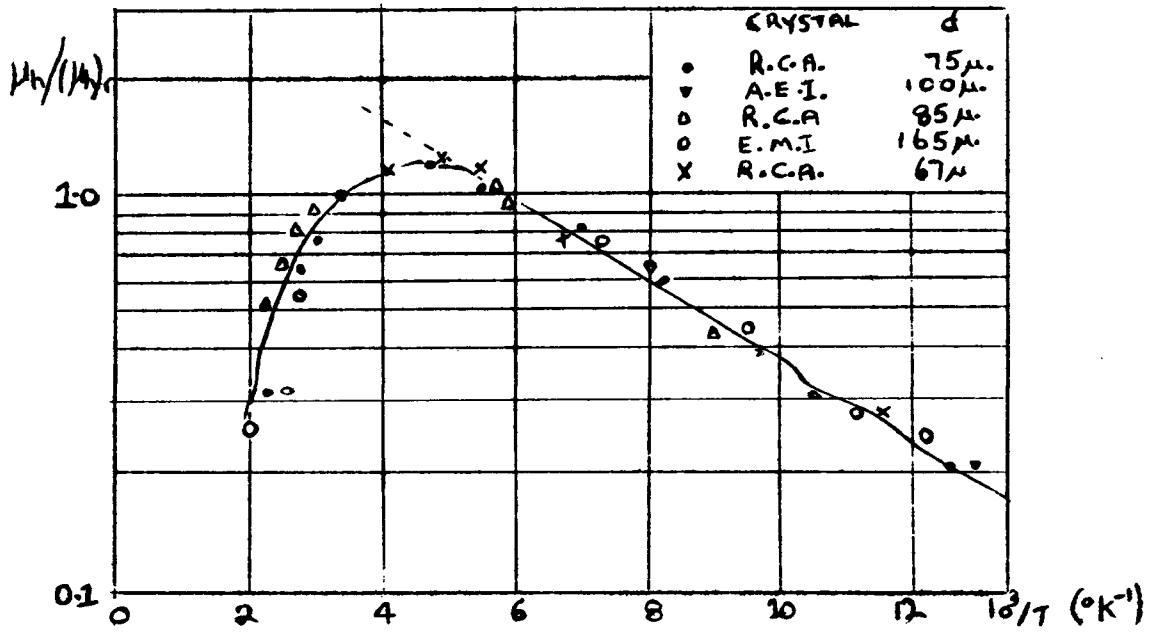

Figure 6: Temperature dependence of the hole drift mobility μ_h, normalised to its room temperature value $(\mu_h)_r$ for five specimens from the sources indicated.

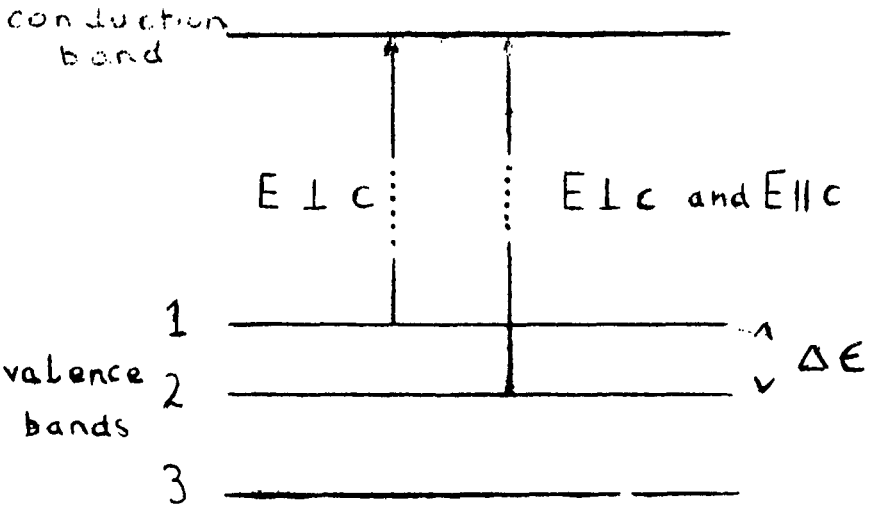

Figure 7: Energy level diagram illustrating the band structure of CdS at k = 000 and the allowed optical transitions.

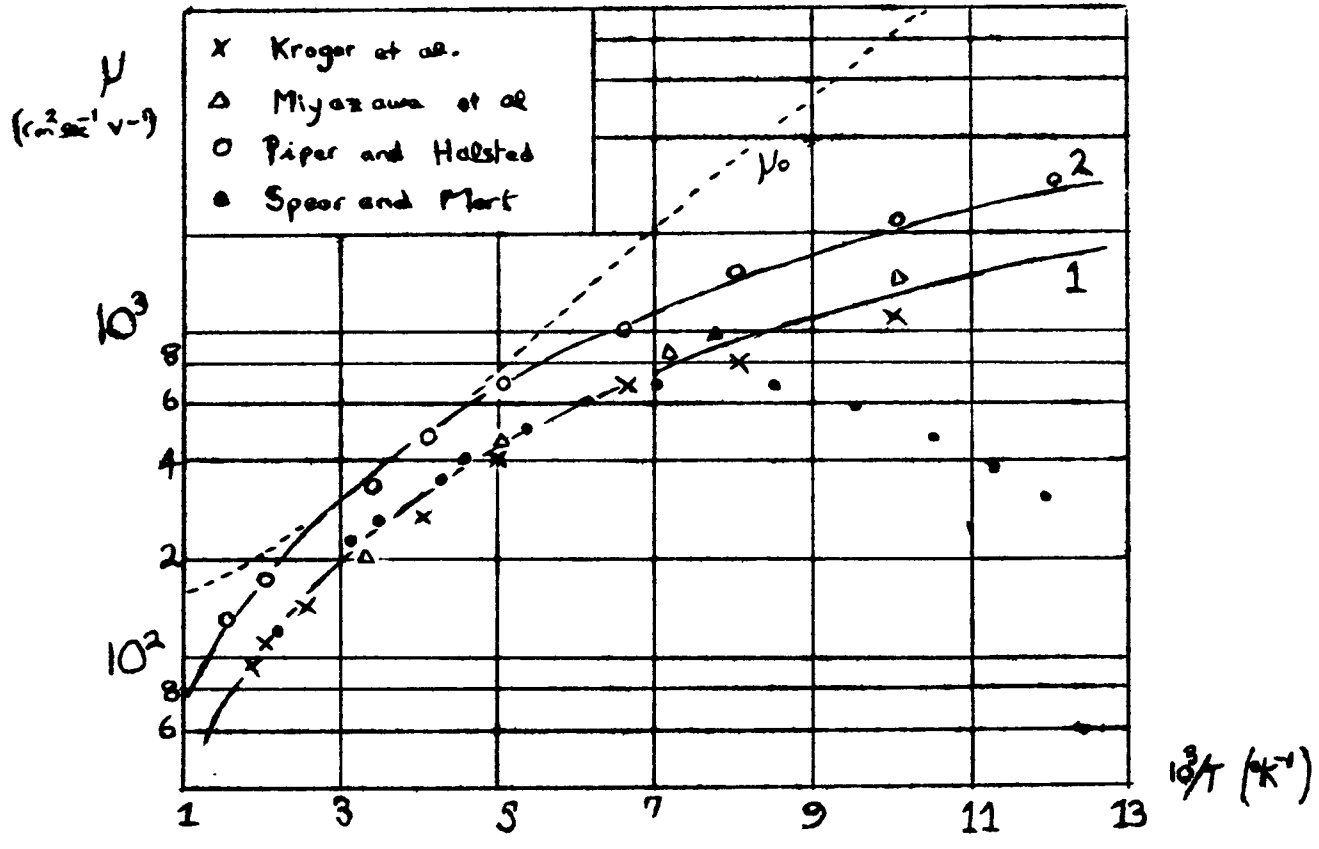

Figure 8: Graph comparing the temperature dependence of the electron drift mobility with Hall mobility data of various authors. The solid lines 1 and 2 are mobility curves determined by acoustic scattering with $b = 1.28 \times 10^6$ and 2.0×10^6 cm $sec^{-1} v^{-1} \sigma_K^{3/2}$ respectively. μ_o represents the mobility determined by polar optical mode scattering.

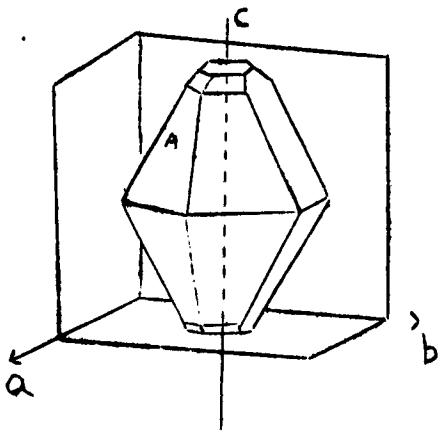

Figure 9: Common habit of thick orthorhombic S crystals.

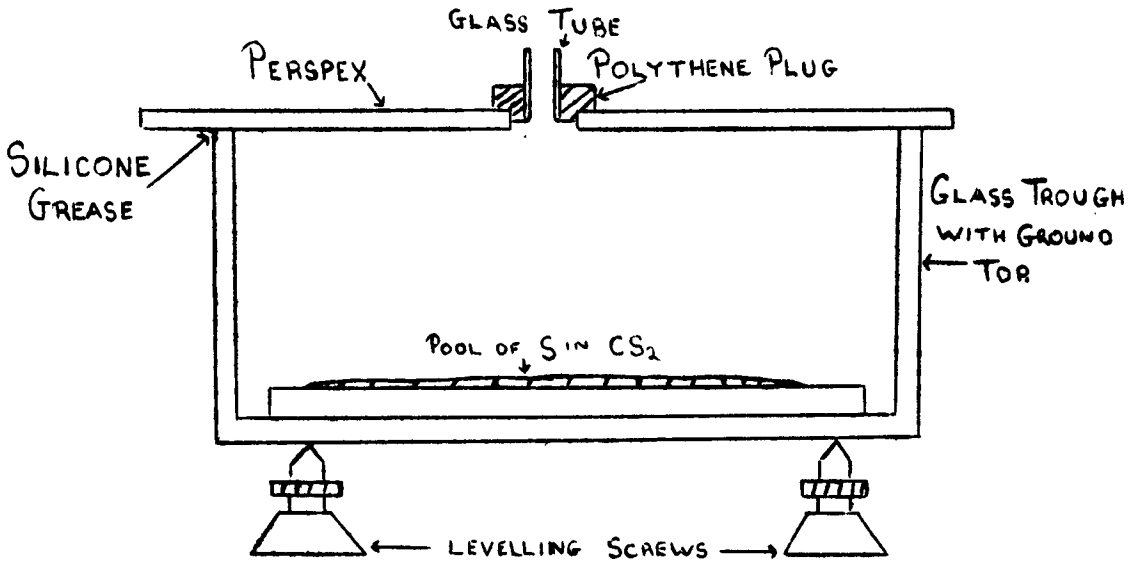

Figure 10: Method of growing thin plate crystals from solution

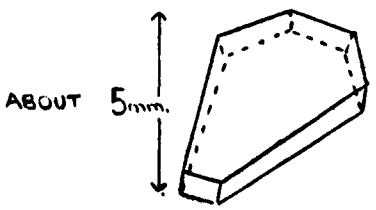

Figure 11: Typical thin plate crystal. The c-axis makes an angle of 18° 20' with the crystal face which corresponds to Face A in Figure 9.

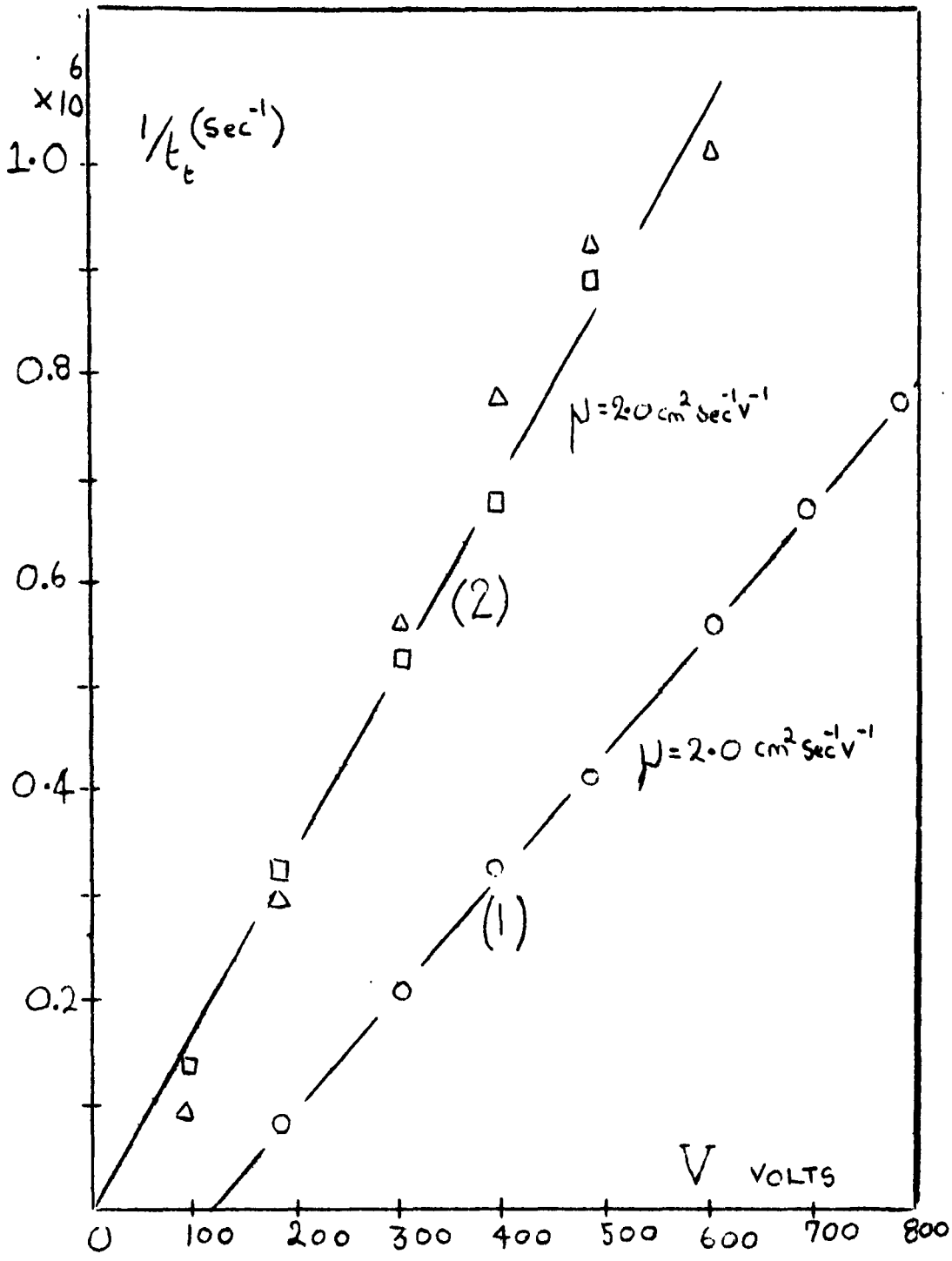

Figure 12:

○ Natural faces d = 429μ curve 1.

△ Bottom Ground d = 339μ) curve 2.

□ Top Ground d = 330μ)

Graph of $1/t_t$ against applied voltage for specimen 823 and its dependence on surface treatment.

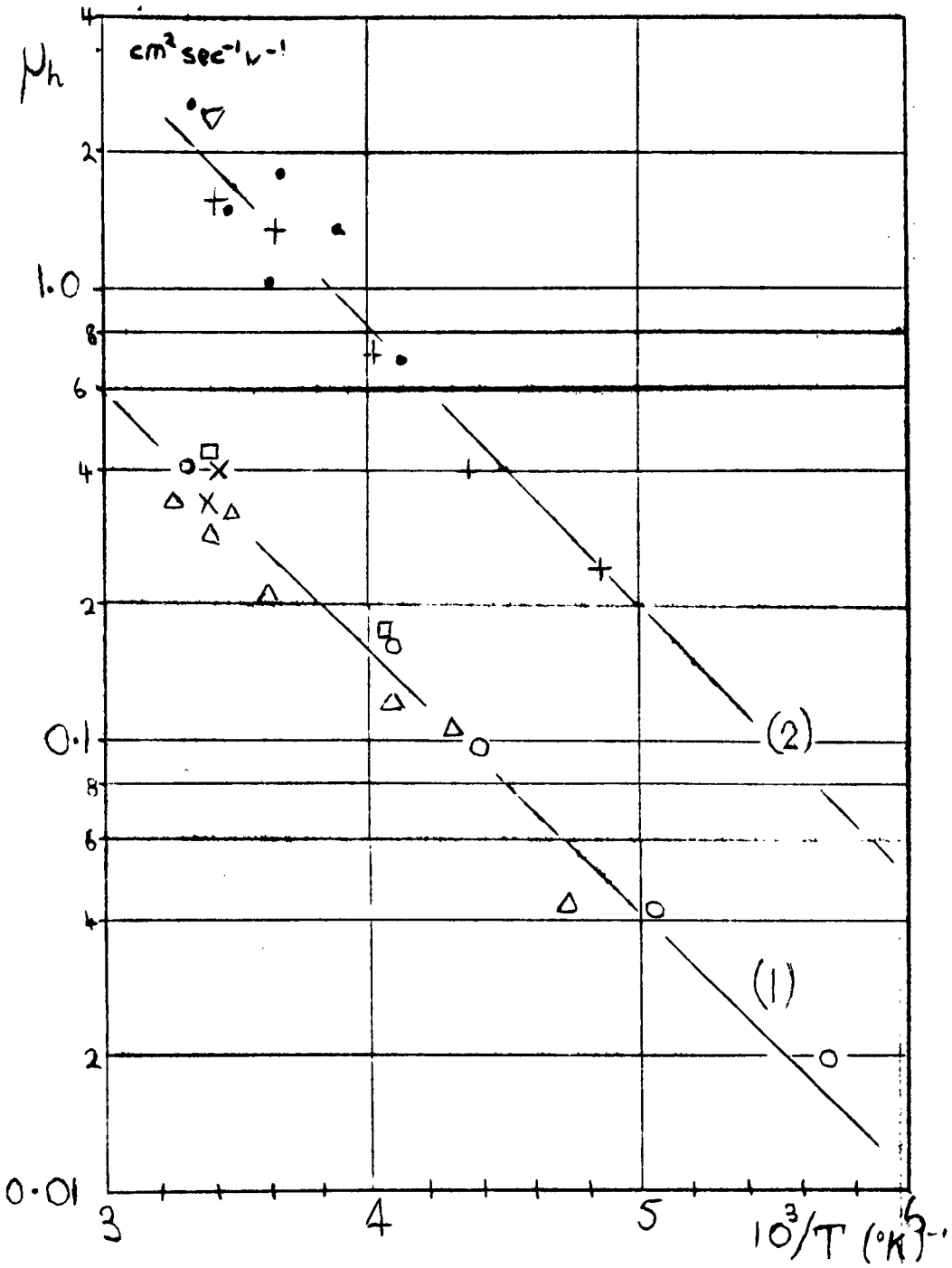

Figure 14: The temperature dependence of the hole mobility.

(1)
- (○ S11, ground, 180μ thick, grown from ultra-pure reagents.
- (□ S12, natural faces, 370μ thick, grown from ultra-pure reagents.
- (△ S13, ground, 150μ thick, grown from ultra-pure reagents.
- (× S14, top ground, 130μ thick, grown from ultra-pure reagents.

(2)
- (+ S16, natural faces, 450μ grown from laboratory reagents.
- (• S4, natural faces, 250μ grown from laboratory reagents.
- (▽ S23, ground, 330μ grown from laboratory reagents.

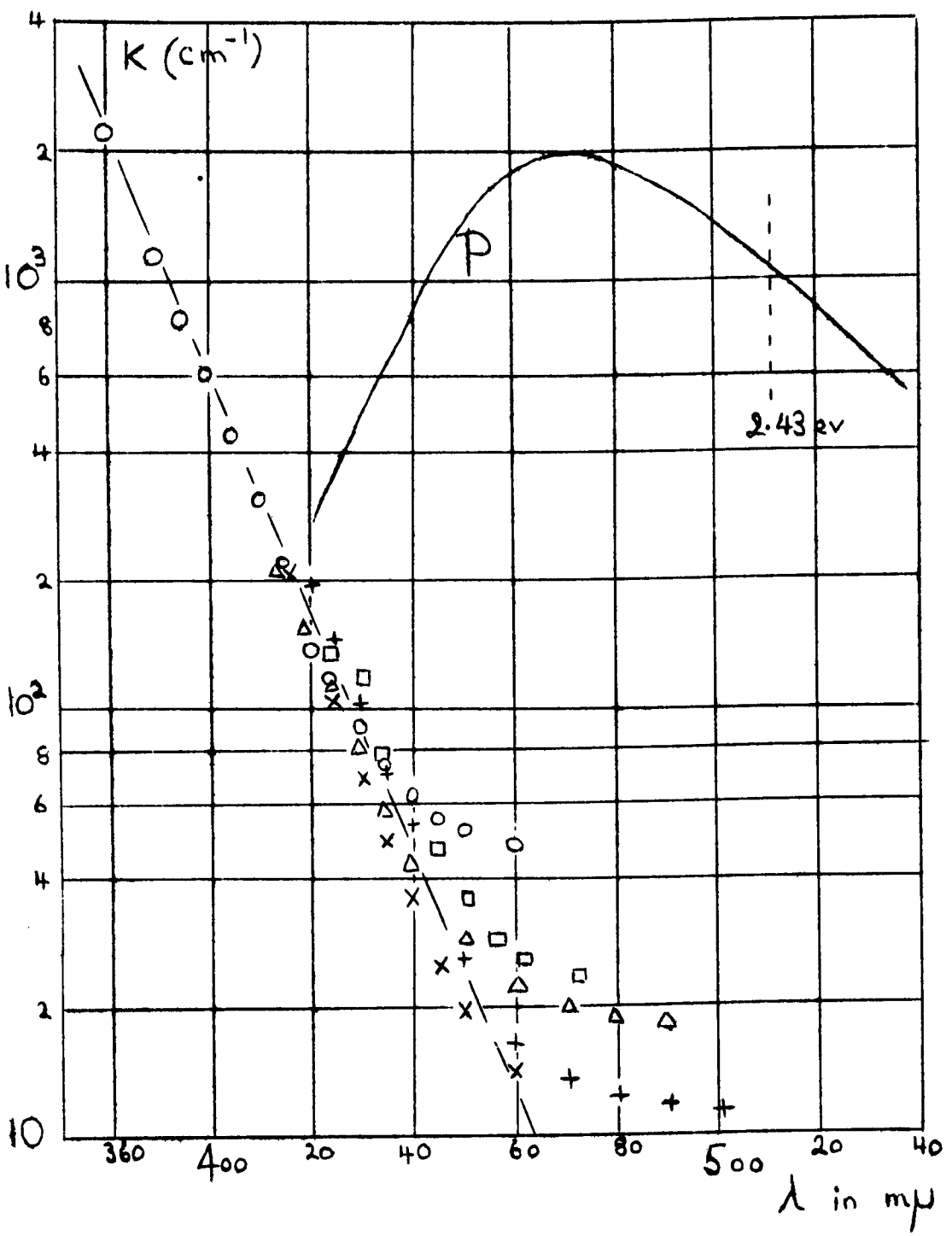

Figure 15: Spectral dependence of the absorption coefficient in rhombic S for a number of specimens between 75μ and 750μ thick. No reflection correction has been applied.

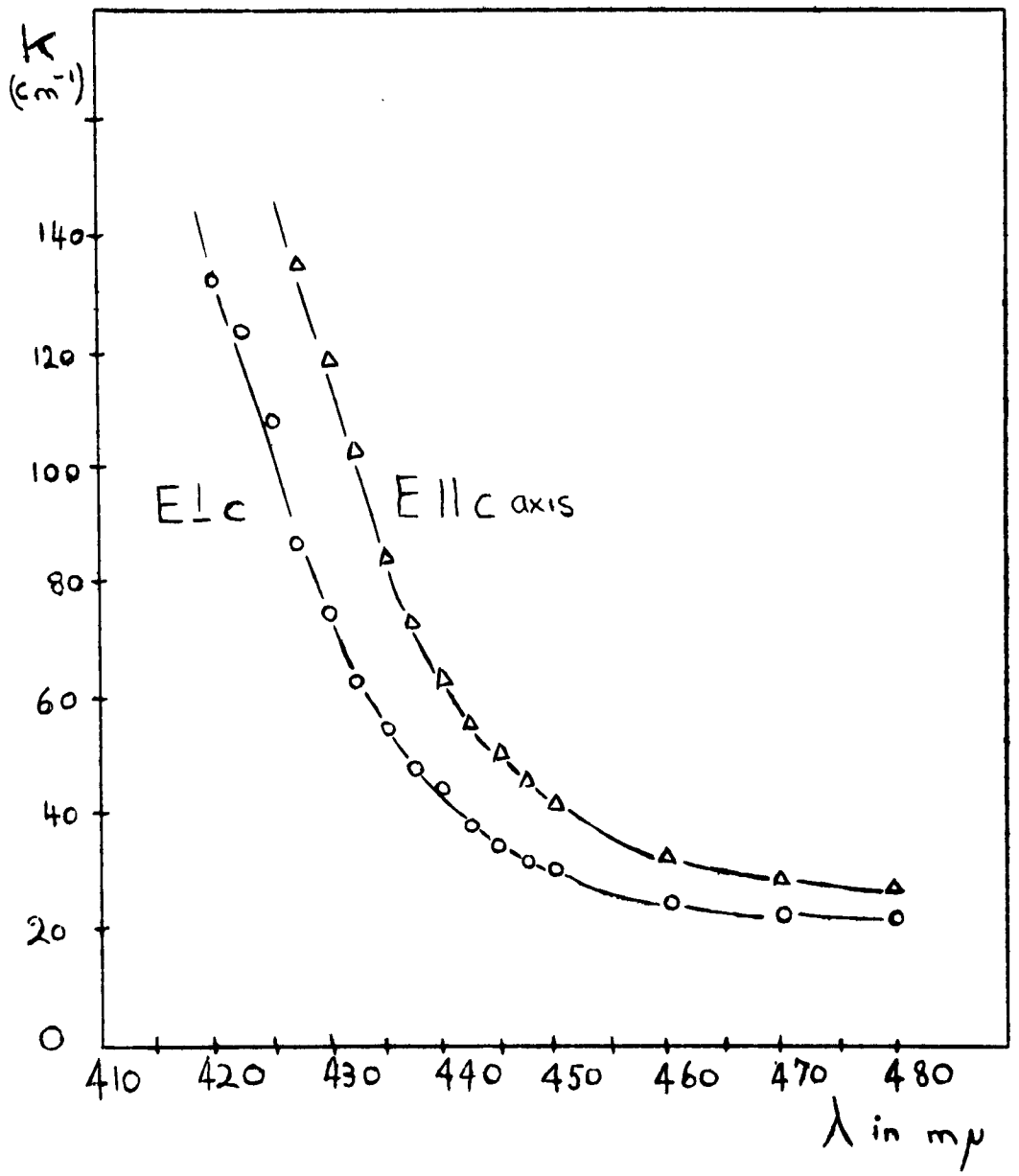

Figure 16: Dependence of the absorption edge on the plane of polarisation of the incident light.